Anal. Bioanal. Electrochem., Vol. 6, No. 4, 2014, 403-421

Analytical & Bioanalytical Electrochemistry

www.abechem.com

Full Paper

Synthesis, Characterization, Conductivity and Antibacterial Activity of Ethyl Cellulose Manganese(II) Hydrogen Phosphate

Tanvir Arfin* and Chintan Kumar

Department of Chemistry, Uka Tarsadia University, Maliba Campus, Gopal Vidyanagar, Bardoli-394350, India

* Corresponding Author, Tel. +91-7878366678

E-Mail: tanvirarfin@ymail.com

Received: 8 May 2014 / Accepted: 11 August 2014 / Published online: 31 August 2014

Abstract- The ethyl cellulose manganese(II) hydrogen phosphate was synthesised by sol-gel method using various 1:1 electrolytes at different temperature and concentration. These materials were characterized by using Fourier transform infrared (FTIR) spectroscopy, Ultraviolet-visible (UV-vis) spectroscopy and pH meter. This material refers a new class of material as it contains both organic that is a polymer and inorganic parts along with the improved chemical as well as mechanical stabilities. The material conductivity generally decreases in the order $K^+ > Na^+$ for 1:1 electrolyte solution. This study displayed the applications of conductivity of materials in the varied field of science. The material exhibited inhibitory results against gram positive bacteria like Staphylococcus aureus (MSSA-22) and gram negative bacteria like Escherichia coli (K-12), and it marked the enhancement in the effectiveness of the antibacterial agent.

Keywords- Ethyl cellulose manganese(II) hydrogen phosphate, Material conductivity, Antibacterial activity

1. INTRODUCTION

The unique properties that added the challenge of research have increased the scientific and technological demand for novel materials. Due to the exceptional properties that are

apparently different from its bulk material the organic-inorganic materials have caught the interest of researchers [1,2]. Now a day synthesis of advanced functional materials in nano-scale is one of the major fields of interest found among the research group [3]. For the fabrication of a structure a nano-particle is the recommended and basic component, the bulk metals and metallic particles have different physical and chemical properties such as lower melting points, higher specific surface area, specific optical properties, mechanical strength, and specific magnetization that is enthralling in various industrial applications [4,5]. The specific optical property is the most appreciated property having fundamental attraction and it is one of the characteristic of nano-particle [6].

Cellulose a complex carbohydrate is the most plentiful and renewable bio-polymeric material found in nature which is widely used in membranes and pharmaceuticals owing to its properties such as that of non-toxicity, biocompatibility, and mechanical strength [7-9]. But yet it is observed that cellulose does not melt and dissolves in normal organic solvent due to its strong inter- and intra-molecular hydrogen bonds that have been divulged experimenting. It was noted that the chemical modifications of cellulose were cited in an autarky way [10-12]. Hydrophobic matrix carrier ethyl cellulose (EC) was used as the admirable release carrier [13,14] that was commonly employed in pharmaceutical and biomedical industries for its qualitatively high biocompatibility and biodegradability which was able to cope up with the results.

A manganese phosphate was used as catalysts for the oxidation of methyl mandelate [15] and of adonitol to ribose [16] for a major period of time. It also has some valid coating properties and imparts a major role in the corrosion protection of mild steels [17] and as the intermediate coverage layer just before the extreme painting of automobile iron castings [18]. Along with the electrochemical properties of manganese phosphate, it is bestowing industrial interest as well [19,20]. There are two types of hydrogen bonds in $Mn(HPO_4).2H_2O$ which are connected in the crystal lattice in a diverse, fickle manner: the first one is formed by the POH groups and second one—by the water molecules. Hence the characterization of spectroscopy of hydrogen bond seems to be very enthralling and also the correlation of the vibrational and crystallographic data becomes clearly visible [21].

In analytical chemistry, process industry, food analysis and water-quality control, the measurement of electrolyte conductivity (EC) is common trends followed in the present world [22-24]. In pharmacology, blood and urea analysis, and tissue-perfusion measurement and also in the chemical and biological sensing field for the detection of a variety of biochemical species for examples amino acids, proteins, peptides, DNA),explosives and chemical warfare agents, the use of such electrolyte conductivity is noted [25-27]. In general the EC measurements are done by employing the ideally polarisable inert metal electrodes such as platinum or gold which have direct contact with the electrolyte.

In the present study, the composite ethyl cellulose manganese hydrogen phosphate was synthesized by a sol-gel method with different electrolytes in the ratio 1:1 at different temperatures and concentrations for modulating the possible interactions between ethyl cellulose and manganese hydrogen phosphate. By employing 1:3 wt/wt. ratio of binder such as ethyl cellulose and manganese hydrogen phosphate, the composite material was prepared. The values of the material were raised non-linearly with the relation of the square root of electrolyte concentration at various temperature ranges which shows excellent inhibitory results in the two different cultures of bacteria. Such material is expected to show a large number of applications in a self-sufficient way, which makes them to approach in filtration tasks such as beverage, textile industry, medicine, pharmacy, chemical industry, waste water treatment and so on. These applications are very cert due to the various properties such as their high thermal resistance, chemical resistance and the mechanical strength.

2. EXPERIMANTAL

2.1. Synthesis of composite ethyl cellulose manganese(II) hydrogen phosphate

Manganese(II) hydrogen phosphate precipitates were prepared by mixing a 0.2 manganese(II) chloride (99.00%, S.D. Fine-Chem Limited) and a 0.2 M dipotassium hydrogen orthophosphate (98.00%, S.D. Fine-Chem Limited) solution which bestow the light white precipitates. The pH of the mixture was maintained as 1.0 by adding dilution hydrochloric acid ((35.40%, S.D. Fine-Chem Limited)) with continuous stirring and the left over precipitates were kept for overnight at room temperature [28]. The supernatant liquid was poured out and the filtration of precipitate was done to remove excess acid and the resulting solid residue was washed with de-ionized water. The solid residues were later dried at 80 °C in an oven and then grounded to a fine powder with the help of a pestle and mortar, and the free flowing powder was finally sieved using an 85 μm sieve. The obtained chemical formula is given below as:

$$MnCl_2 + K_2HPO_4 \rightarrow MnHPO_4 + 2KCl$$

The manganese(II) hydrogen phosphate and ethyl cellulose powders were mixed thoroughly through a pestle and mortar for major period of time. The mixture was placed in an oven having a temperature of 80 °C for an hour to equilibrate the reaction [29]. The materials that was prepared by embedding 25% ethyl cellulose with manganese(II) hydrogen phosphate had the highest mechanical stability and gave reproducible results. And the material with greater amounts (>25%) of ethyl cellulose did not give a reproducible results but the one with lesser amounts of ethyl cellulose (<25%) were found to be unstable. For the preparation of the material, 63 mg of ethyl cellulose and 187 mg of manganese(II) hydrogen phosphate was utilized as a mixture. All such materials were prepared by compressing the

powder of the composite into tablets by employing a Tablet compression (Mini press 1 station, Rimek) as shown in Fig. 1. and Fig. 2.

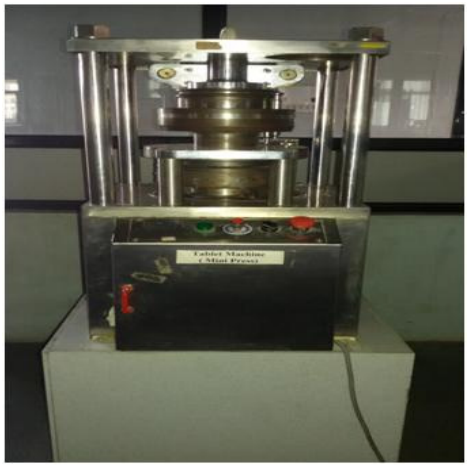

Fig. 1. Tablet compressing Machine

Fig. 2. Powder converted into tablet by tablet compressing machine

The tentative structure proposed is given below:

$$Mn(HPO_4).nH_2O + [C_6H_7O_2(OC_2H_5)_3] \rightarrow Mn(HPO_4).[C_6H_7O_2(OC_2H_5)_3].nH_2O$$

where 'n' represents the number of hydrated water molecules.

2.2. Measurement of material conductivity

For the electrochemical measurements, the test cell used is very similar to that described elsewhere [30,31]. For precaution the materials were tightly clamped between two glass half-cells of the material conductivity. The half-cell volume was taken as 20 mL and the effective material area was noted as 60.13 mm^2. Various electrolyte solutions such as that of chlorides

of K^+, and Na^+ of different concentration have been prepared by using deionised water to minimize the concentration-polarization at the material surfaces where a magnetic stirrer was placed at the bottom of each half-cell and the measurements of the electrolyte solutions were carried out at a stirring rate of 500 rpm [32,33]. PH of the solutions was in the range of 5.5 to 6. The measurements of conductivity were carried out by adopting one of the qualitative methods followed in [34,35] at different temperature range of (5±50)±0.2°C for beguile analysis. The material conductivity was recorded by utilizing an auto ranging digital conductivity meter named as Model No.EQ-667, Equip-Tronics. For each experiment three different reading of the conductivity were taken into account and then the mean was taken as the final output.

2.3. Spectroscopic measurements

Ultraviolet-visible (UV-vis) spectra was obtained by employing a UV-1800 spectrophotometer(Shimadzu). The aqueous suspension of material was used as the UV-vis sample, and the de-ionized methanol was used for the reference. On an Alpha-FTIR spectroscopy (Bruker), a FT-IR spectrum of sample was recorded. The spectrum of the sample was finalized after taking out the average of 200 scans between 4000 and 600 cm^{-1} with a resolution of 4 cm^{-1} which was corrected against the background spectrum at ambient temperature during the complete experimentation process.

2.4. Antibacterial activity of material

By using broth dilution method and disc diffusion method, the antibacterial study of ethyl cellulose manganese(II) hydrogen phosphate was analysed in vitro against two gram positive bacteria Staphylococcus aureus (MSSA-22) and two gram negative bacteria Escherichia coli (K-12) strains [36,37]. Test strains were cultured in Nutrient Broth containing various substances such as Lab-Lemco powder 0.1% (w/v), yeast extract 0.2% (w/v), peptone 0.5% (w/v), sodium chloride .5% (w/v). The pH value was maintained to be 7 and checked after addition of each agent and result of it was not altered. Bacteria were maintained on Mueller Hinton Agar medium containing meat infusion 30% (w/v); casein hydrolysate 1.75% (w/v); starch 0.15% (w/v); agar–agar 1.7% (w/v).

2.4.1. Broth dilution method

Broth dilution assays were carried on in the culture tubes having Nutrient Broth inoculated with 10^7–10^8 CFU/ml of bacterial strain and the ethyl cellulose manganese(II) hydrogen phosphate in the wide range of concentrations at 100–1000 μg/ml. The tubes were incubated for 24 h at 37 °C and visible culture growth was recorded with consistency and atonements. The Minimum Inhibitory Concentration (MIC) was defined as the minimum

concentration of the ethyl cellulose manganese(II) hydrogen phosphate where the culture growth did not occur at all. For the next, bacterial cultures were plated on non inhibitory solid media (Mueller Hinton agar) and incubated at 37 °C for 24 h to detect the survivors and on such basis the Minimum Bactericidal Concentration (MBC) was measured as the lowest concentration of the ethyl cellulose manganese(II) hydrogen phosphate which also resulted in no growth. Each experiment was repeated thrice for better results with precaution.

2.4.2. Disc diffusion method

The screening for antibacterial activities are carried out using sterilised discs (5 mm), where the sterilised disk was soaked previously in 0.2 M concentration of the test complex and then dried at 70 °C for 6 h. All the strains for testing were incubated and activate at 37 °C for 24 h inoculation and later in Nutrient Broth for 48 h. Inoculums containing 10^7–10^8 CFU of bacterial cells was spread on Mueller–Hinton Agar plates (100 µL inoculum for each plate). The discs that was soaked with CSP composite were placed on the inoculated agar by compressing with slight force and incubated at 37 °C for 24 hr. Tetracycline (30ug/disk, Hi-Media) was used as control for disc diffusion method. The inhibition zone was measured (in mm) after 24 h. Each experiment was performed thrice for the appropriate results.

3. RESULT AND DISCUSSIONS

3.1. Spectroscopic Investigations

3.1.1. UV-visible absorbance spectral study

The electronic absorption spectrum of the ethyl cellulose manganese(II) hydrogen phosphate was observed at different range of 270-200 nm with a length of 1 cm quartz cell path along it. Fig. 3 shows the electronic absorption spectrum of ethyl cellulose manganese(II) hydrogen phosphate where the peak was observed in the middle ultraviolet range generally at 300-200 nm. A 3 mL volume of sample was investigated separately at room temperature with the wavelength that have a maximum absorption of 228 nm for ethyl cellulose manganese(II) hydrogen phosphate which is as shown in Fig. 3. An absorption peak appears at 228 nm which attributes to $\pi - \pi^*$ transitions in small electronically conjugated domains that is aromatic C-C ring [38].

Table 1. Gaussion curve analysis for the band in spectrum of the sample at 25 °C

System	Area of the curve *(A)*	Width of the curve *(w)*	Centre of the curve (x_c)	y_0	R^2
Sample	44.289 ± 1.522	32.122 ± 0.736	224.220 ± 0.193	0.410 ± 0.018	0.970

The absorption spectra were examined by fitting to the Gaussian function such as $y = y_0 + \left[A/\left(w\sqrt{(\pi/2)}\right)\right]\exp\left[-2\left(x-x_c\right)^2/w^2\right]$, where wavelength and absorbance are denoted by x and y. Table 1 shows the results of the Gaussian analysis for the band in spectrum.

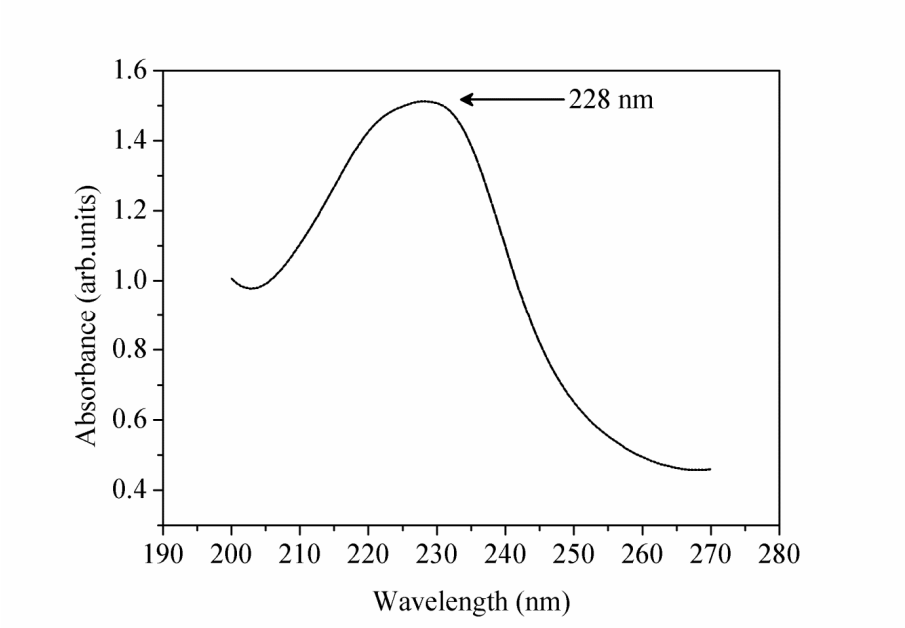

Fig. 3. UV-Vis image of the Ethyl cellulose manganese hydrogen phosphate

3.1.2. Determination of ionization potentials

The empirical equation derived by physicist such as Aloisi and Pignataro was used to calculate the ionization potential of the material ethyl cellulose manganese(II) hydrogen phosphate [39]:

$$I_D(eV) = 5.76 + 1.53\times10^{-4}\nu \quad (1)$$

where ν is the wavenumber in cm^{-1} of the material. The value of ionization potentials estimated is given in Table 2. The wavelength of the absorption which is maxima $(\lambda_{max} = x_c)$ and the corresponding transition energy $(h\nu)$ is summarized in Table 2.

Table 2. Various parameters of the sample at 25 ℃

System	$\lambda(nm)$	$h\nu(eV)$	$I_D(eV)$	$f\times10^5$	$\mu_{EN}(Debyes)$	$R_N(eV)$	$E(nm)$
Sample	228	5.390	12.470	0.025	0.0102	2.562	5.445

3.1.3. Determination of oscillator strength (f)

For expressing the transition probability of the bands [40] of the material the oscillator strength (f), having the dimensionless quantity was employed. From the absorption spectra, the oscillator strength was generated and the oscillator strength f was calculated by using the formula given below:

$$f = 4.32\times10^{-9}\int \varepsilon.d\nu \tag{2}$$

where $\int \varepsilon.d\nu$ is the area under the curve of the extinction coefficient of the absorption band in question *vs*. the frequency. For the first approximation it is taken as:

$$f = 4.32\times10^{-9}\varepsilon\Delta\nu_{1/2} \tag{3}$$

where ε is the maximum extinction coefficient on the band and $\Delta\nu_{1/2}$ is the half-width, i.e., the width of the band at half the maximum extinction. The observed oscillator strength of the band is also listed in Table 2.

3.1.4. Determination of transition dipole moment (μ_{EN})

The extinction coefficient is in relation with the transition dipole which is as depicted below in Eq. (4):

$$\mu_{EN} = 0.0952\left[\varepsilon\frac{\Delta\nu_{1/2}}{\Delta\nu}\right]^{1/2} \tag{4}$$

where $\Delta\nu \approx \nu$ at ε and μ_{EN} is defined as $-e\int\psi_{ex}\sum_i r_i\psi_g d\tau$. And μ_{EN} for sample is given in Table 2.

3.1.5. Determination of resonance energy (R_N)

Briegleb and Czekalla [41] have derived the relation in a theoretical concept which is given as:

$$\varepsilon = \frac{7.7\times10^{-4}}{h\nu/[R_N]-3.5} \tag{5}$$

where ε is the molar extinction coefficient of the material at the maximum range of the absorption, ν is the frequency of the peak and R_N is the resonance energy of the material

showing the ground state, that is a contributing factor for the stability constant of the material. The value of R_N for the material that has been studied is given in Table 2.

3.1.6. Determination of transition energy (E)

The transfers of lone pair of electron have arisen because of the hydrogen bonding between the materials which were remarketed by the existence of new band in the material. The energy was calculated by empowering the equation that was derived by Briegleb [42].

$$E = \frac{1243.667}{\lambda} nm \tag{6}$$

where λ is the wavelength of the band of the material and data is catalogued in Table 2.

3.2. FTIR study

FTIR spectra was analysed to check the presence of functional groups in the sample which was revealed in Fig. 4 that showed distinct peaks at 2975, 1455 and 1385 cm^{-1}, resembling CH stretching, CH_3 and CH_2 bending, respectively [43]. The strong peak at 1065 cm^{-1} was in touch to C-O-C stretching in the cyclic ether of ethyl cellulose [44]. The bands at 870, 772 and 538 cm-1 were ascribed to the vibration of PO_4^{3-} [45]. A group of sharp peaks in the region of 583 cm^{-1} symbolised to the superposition of metal–oxygen stretching vibration [46]. A less broad peak around in the region 1014 cm^{-1} was mainly because of the presence of HPO_4^{2-} [45].

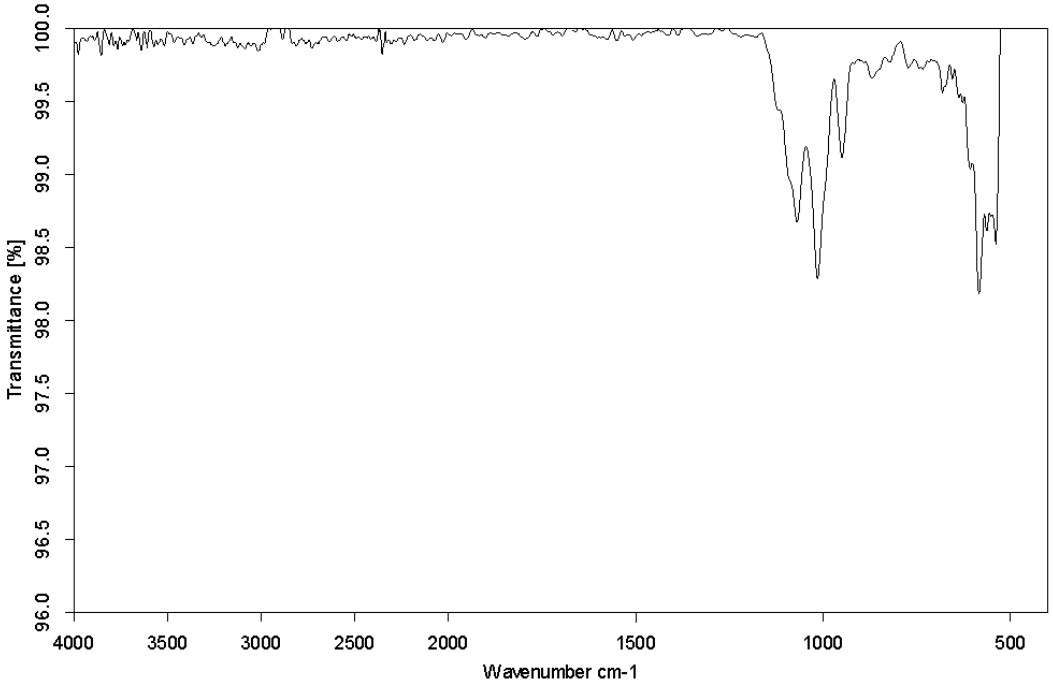

Fig. 4. FTIR image of the Ethyl cellulose manganese hydrogen phosphate

3.3. Antibacterial study

The antibacterial studies on ethyl cellulose manganese(II) hydrogen phosphate was done for investigating the antibacterial action by using disk diffusion method [36,37] against two gram positive bacteria Staphylococcus aureus (MSSA-22) and two gram negative bacteria Escherichia coli (K-12). Tetracycline was used for the control method as the standard drug for comparison between antibacterial properties of ethyl cellulose manganese(II) hydrogen phosphate. The results and noted data of such study are given in Table 3. The freshly synthesized ethyl cellulose manganese(II) hydrogen phosphate showed remarkable inhibitory effects in comparison to the growth of the tested bacterial strains. The antimicrobial property of various synthetic molecules was examined by different researchers, such as antimicrobial activities of 1,6-bis(benzimidazol- 2-yl)-3,4-dithiahexane ligand was found in similar manner [47]. The data given in table 3 depicted that the ethyl cellulose manganese(II) hydrogen phosphate exhibit more frequent activity with Staphylococcus aureus when compared to the Escherichia coli. The result clearly shows that the ethyl cellulose manganese(II) hydrogen phosphate is more active against all tested bacterial strains than tetracycline which was used as a control method and finally suggested that it can be used as potent antibacterial agent.

Table 3. Antibacterial activity of ethyl cellulose manganese(II) hydrogen phosphate

Diameter of zone of inhibition in mm at 100µg/ml and DMSO as control		
Bacteria	ethyl cellulose manganese(II) hydrogen phosphate	Tetracyline
Staphylococcus aureus	15.3±1.25	14.5±0.88
Escherichia Coli	13.9±0.75	12.5±0.23

3.4. Conductivity study

The variations of the conductivity along the material corresponding to different 1:1 electrolyte concentration at room temperature are shown in Fig. 5. The electrolytic conductance is said to increase with the decrease in concentration because conductance of ions is followed by the presence of ions in the solution. The greater the number of ions, the greater will be the conductance. As with dilution, more number of ions is produced in solution, so the conductance is found to increase on dilution.

The above noted statement is in relation with the findings and observational reading of Arfin *et al.* [28,29] that is for the membranes with alkali chlorides

The conductivity of the material was said to decrease in order $K^+ > Na^+$ for the 1:1 electrolyte solution which was harmony to the decrease in size of the cation that was mentioned by *Beg et al.* [48]. This sequencing have shown the result and it later confirmed

that the material was weakly charged [49] and the ionic species retain their hydration shells which was least partial in nature [50].

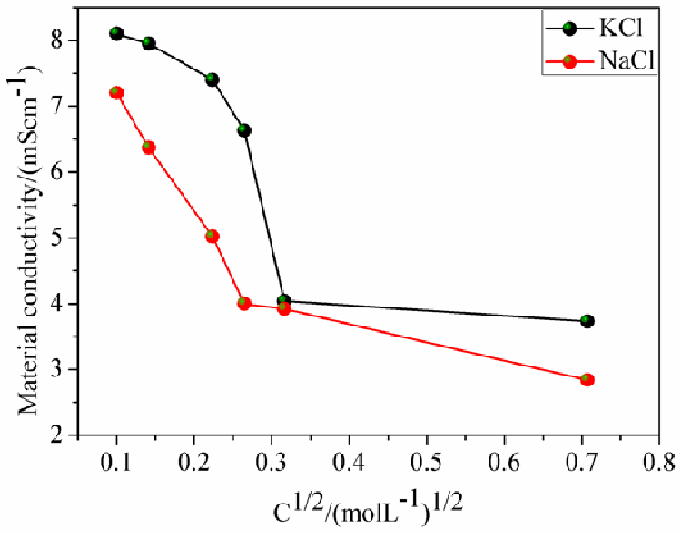

Fig. 5. Plot of material conductivity *vs.* concentration for the Ethyl cellulose manganese hydrogen phosphate using 1:1 electrolytes at 25±0.1°C

It was noticed that on dilution, conductivity of the material decreases but volume containing one mole of an electrolyte increases which confirmed that the increase in volume on dilution is much more than the decrease in conductivity. As a result of which the molar conductivity also increases with dilution. When the strong electrolytes are studied, molar conductivity is found to increase slowly with dilution in it. Molar conductivity follows the tendency to approach a certain limits in the value when the concentration approaches zero i.e., when the dilution is infinite. Thus molar conductivity at infinite dilution is termed as molar conductivity when the concentration moves towards zero. It is denoted by Λ_m^∞. Thus,

$$\Lambda_m = \Lambda_m^\infty \tag{7}$$

when C→0 at infinite dilution

It is also noticed that the variation of molar conductivity with concentration is given by the expression mentioned below:

$$\Lambda_m = \Lambda_m^\infty - A\sqrt{C} \tag{8}$$

Where A is a constant and Λ_m^∞ is called molar conductivity at infinite dilution. The above mentioned equation is called Debye Huckel Onsager equation which is holding good at low concentration.

By plotting the values of Λ_m against square root of concentration $\sqrt{C}$, the variation of molar conductivity with concentration can be studied and analysed. The plots of variation of molar conductivity with $\sqrt{C}$ for KCl and NaCl are given in Fig. 6. It was observed that the variation of Λ_m with concentration, $\sqrt{C}$ was very small so that the plots was extrapolated to zero concentration. The intercept gives the limiting value of molar conductivity when the concentration reached to zero, which was called as molar conductivity at infinite dilution, Λ_m^{∞}. The slope of the line is equal to –'A'. It was remarketed that the value of constant A for a given solvent and temperature was dependent on the type of electrolyte generally the charges on the cation and anion produced on the dissociation of the electrolyte in the solution.

The number of ions did not increase with dilution because KCl and NaCl electrolytes was completely ionised in solution at various concentrations. But it was noted that in concentrated solutions of KCl and NaCl electrolytes there exist a strong forces of attraction between the ions of opposite charges which was called as inter-ionic forces. It was because of such inter-ionic forces that the conducting capability of the ions is less in the concentrated solutions. The inter-ionic forces decrease which is resulting in ions becoming far apart from one another with dilution which finally leads the molar conductivity to increase with dilution. The inter-ionic attractions become negligible, when the concentration of the dilution becomes extremely low and the molar conductance approaches the limiting value called molar conductance at infinite dilution. The values for molar conductivity of material is given in Table 4. The molar conductivity was found to be $K^+ > Na^+$ for a 1:1 electrolyte solution. Thus, this type of behaviour is also observed in the previous paper as well [28,29].

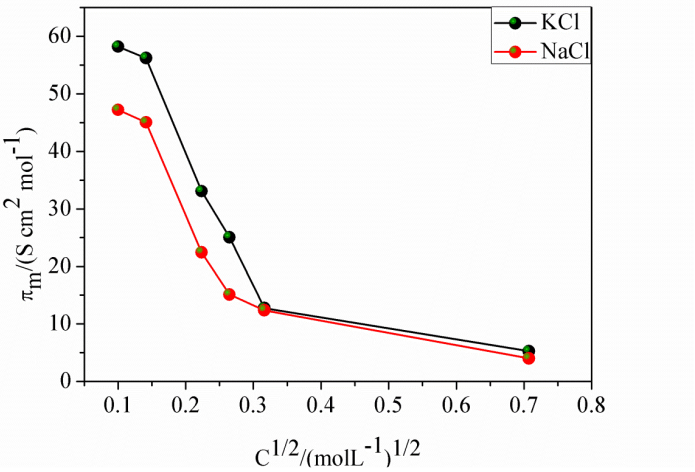

Fig. 6. Plot of material molar conductivity *vs.* concentration for the Ethyl cellulose manganese hydrogen phosphate using 1:1 electrolytes at 25±0.1°C

Table 4. Derived values for Ethyl cellulose manganese hydrogen phosphate parameters of Λ_m^{∞} using 1:1 electrolytes at 25±0.1°C

Electrolytes (mol L^{-1})	Λ_m^{∞} (S cm^2 mol^{-1})	-*A*
KCl	93.975±6.885	84.586±27.196
NaCl	76.614 ±6.130	66.347±23.808

Arrhenius proposed a quantitative relationship between rate constant and temperature as which is as given below [51]: E_a

$$\Lambda_m = \frac{P}{T}\exp\left(\frac{-E_a}{RT}\right) \tag{9}$$

The above equation is called Arrhenius equation in which P is constant and is known as Arrhenius factor or frequency factor. It is also called pre-exponential factor which is a constant specific to a particular reaction. This factor is in relation with many effectively oriented collisions occurring in that specific reaction. E_a is the activation energy which resembles the minimum energy that is possess by the reacting molecule before undergoing a reaction. Both P and E_a are basic characteristics of the reaction which are collectively called Arrhenius parameters. The factor $\exp\left(\frac{-E_a}{RT}\right)$ is corresponding to the fraction of molecules having energy greater than E_a , T is the absolute temperature and R is the gas constant.

Taking logarithm, Eq. (9) may be written as

$$\ln \Lambda_m T = \ln P - \frac{E_a}{R}\times\frac{1}{T} \tag{10}$$

Converting to common logarithm, we get

$$2.303\log \Lambda_m T = 2.303\log P - \frac{E_a}{RT} \tag{11}$$

$$\log \Lambda_m T = \log P - \frac{E_a}{2.303RT} \tag{12}$$

It is quite obvious from the equation that the value of activation energy, E_a increases, the value of Λ_m decreases which finally results in decrease in the reaction rate.

The activation energy can now be calculated from Eq. (12). The equation is in form $y = mx + c$ which represent that it is a straight line. When $\log \Lambda_m T$ is plotted against $\frac{1}{T}$, we

get a straight line as shown in Fig.7. The intercept of this line is equal to $\log P$ and slope is equal to $-\frac{E_a}{2.303R}$. Therefore,

$$Slope = -\frac{E_a}{2.303R} \tag{13}$$

The activation energy can be calculated by knowing the value of slope and gas constant R which is as given below:

$$E_a = -2.303R \times Slope \tag{14}$$

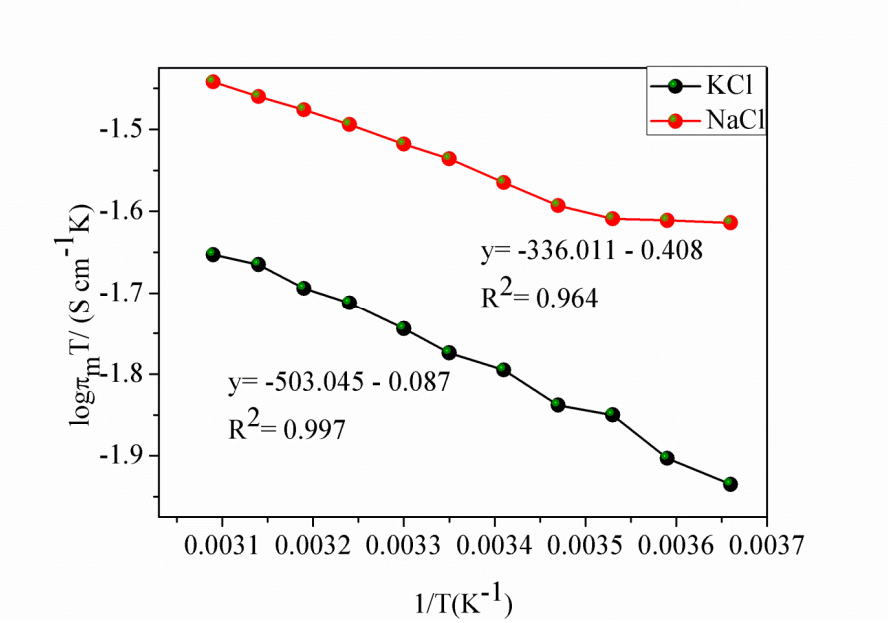

Fig. 7. Plot of material conductivity *vs.* temperature for the Ethyl cellulose manganese hydrogen phosphate using 0.5 M of 1:1 electrolytes at (25-50) ±0.1°C

With the rise in the temperature the material conductivity of an electrolyte is basically found to increases which were resulted experimentally. The material conductivity of a KCl and NaCl electrolyte was dependent on two factors such as: (a) the number of ions present in unit volume of solution; and (b) the speed at which ions move towards the electrodes. The first factor remains the same at the respective temperature for a particular electrolyte which proves that the increase in material conductivity with rise in temperature is due to the influence of the second factor. As the temperature rises, the viscosity of the solvent (water) decreases making the ions to move freely towards the electrodes. The values of conductivity

lie in the order of 10^{-3} Scm^{-1}, resembling that the material is generally under the region of semi-conductor [52].

The minimum amount of energy that is required for an electron to break free from its bound state is called as band gap. When the band gap energy is meeting, the electron is thrilled into a free state which helps in participation of conduction. At the place where the electron was bound, a hole is formed which also leads to participates in conduction. It is symbolising one of the significant specific optical properties of inorganic semiconductors which can expressed generally in a peculiar way as given below [51]:

$$\Lambda_m = \frac{P}{T}\exp\left(\frac{-E_g}{2\kappa T}\right) \tag{15}$$

As the factor of $(1/2)$ in the exponent appears with inorganic semiconductors, all the possible distributions of electrons in the conduction band are independent of the distributions of holes in the valence band normally which is in accordance with the fact proved above.
From Eqs. (9) and (15), we can get

$$E_a = \frac{E_g}{2} \tag{16}$$

Hence, it has been derived that the conductivity is thermally activated with activation energy which is equal to the half of the band gap.

The activation energy (eV) was estimated from the slope of Arrhenius plots for 1:1 electrolyte solution by employing the linear regression method in accordance with the equation given above and is listed in Table 5. It was observed that the activation energy was in close relation with the electro-negativity of the metal ions and both of them were dependent on each other. With a decrease of the electro-negativity of metal ion, the activation energy is also found to be increased which showed that both were inversely proportional to each other as well.

Table 5. Activation energies and band gap energies of conduction for the Ethyl cellulose manganese hydrogen phosphate using 0.5 M of 1:1 electrolytes at (25-50)±0.1°C

Electrolyte (mol L^{-1})	Activation energy (eV)	Band energy gap (eV)
KCl	0.099	0.198
NaCl	0.066	0.132

The variation of the activation energy in accordance with the material and different 1:1 electrolyte concentration at room temperature are shown in Fig. 8. It shows that the activation energy depends on the electrolyte concentration which increases with an increase in the concentration because of the nature of the sovent. For such electrolytes at a particular concentration, it is following the order generally $K^+>Na^+$ and are analogous to the sequence of crystallographic radii of the alkali metal like that of cations. The motion can be enhanced by the segmental mobility of the polymer when the penetrating species moves in a polymer substance which is generally containing relatively small amount of water, where the diffusibility is dependent on the probability of the segment that is making a hole which is very big to be accommodated in a penetrate species in its specific surrounding [53].

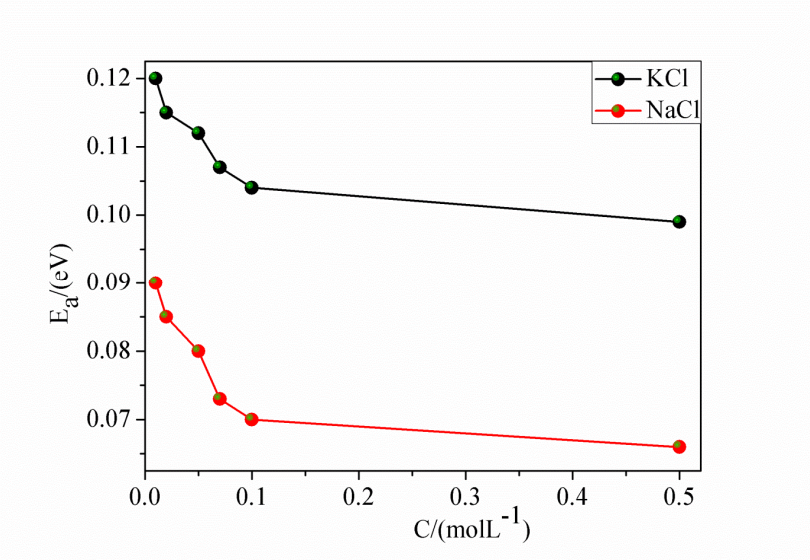

Fig. 8. Plot of activation energy *vs.* concentration for the Ethyl cellulose manganese hydrogen phosphate using 1:1 electrolytes at 25±0.1°C

3.5. pH study

The pH response profile for the maerial was analysed by employing (1×10^{-2} mol L^{-1}) electrolytes solution on the pH range in between 1.0–12.0. The pH was maintained by inserting few drops of hydrochloric acid (0.1 M) or sodium hydroxide (0.1 M) into the solutions. The influence of the pH response on the composite material electrode is shown in Fig. 9.

From the figure it is clear that the potential remains constant from pH 4.0 to 8.0, beyond which some drifts in the potentials were observed which was very comprehensive. The drift at higher pH values was mainly because of the formation of some Hydroxyl complexes of cations the solution. At the lower pH values, the potentials was found to be increased, which

indicated that the material responded to protonium ions, that resulted in the extent protonation of phosphorus atoms of the phosphate. On the other hand, at lower pH values H_3O^+ ions starts to contribute to the charge transport process by the material which led to the cause of interference [54].

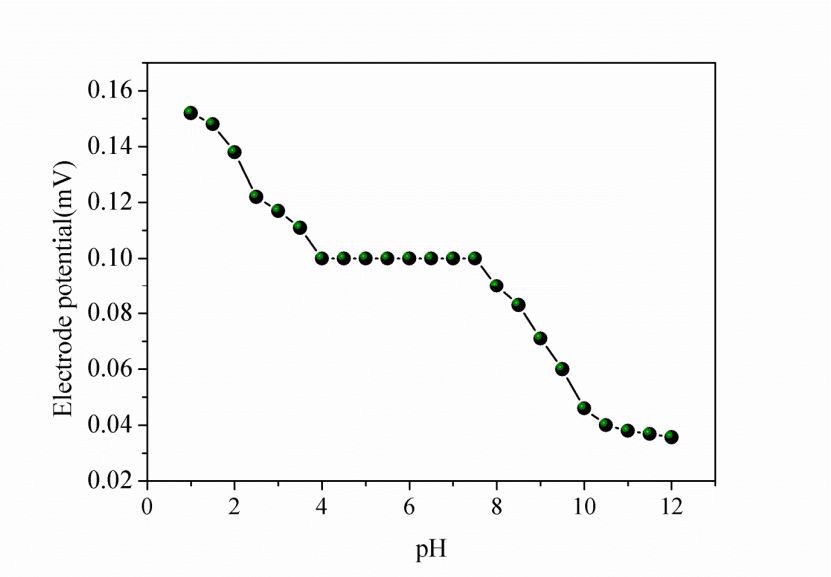

Fig. 9. the effect of pH of the KCl solutions (1×10^{-2} mol L^{-1}) on the potential response of the ethyl cellulose manganese hydrogen phosphate

4. CONCLUSION

The ethyl cellulose manganese hydrogen phosphate composite material is mechanically as well as chemically stable. The new materials imbibed have exerted an important inhibitory activity against the growth of the tested bacterial strains where the data revealed that materials have qualitative influence on the antibacterial profile of gram positive bacteria like Staphylococcus aureus (MSSA-22) and gram negative bacteria like Escherichia coli (K-12).The data clarified that the material has produced the marked enhancement and development in the potency as antibacterial agent. All these results proposed that the composite material offer valuable applications in every expected field today.

Acknowledgements

The Director, Department of Chemistry, UTU is thanked for providing research facilities at Physical Chemistry Lab.

REFERENCES

[1] T. Arfin, and N. Yadav, J. Ind. Eng. Chem. 19 (2013) 256.
[2] F. Mohammad, and T. Arfin, Bull. Environ. Contam. Tox. 91 (2013) 689.
[3] T. Arfin, A. Falch, and R. J. Kriek, Phys. Chem. Chem. Phys.14 (2012) 16760.
[4] F. Mohammad, and T. Arfin, Adv. Mater. Lett. 5 (2014) 315.
[5] A. A. Khan, U. Baig, and M. Khalid, J. Ind. Eng. Chem. 19 (2013) 1226.
[6] S. A. Nabi, M. Shahadat, R. Bushra, M. Oves, and F. Ahmed, Chem. Eng. J. 173 (2011) 706.
[7] N. Kar, H. Y. Liu, and K. J. Edgar, Biomacromolecules 12 (2011) 1106.
[8] W. Yuan, J. Zhang, H. Zou, T. Shen, and J. Ren, Polymer 53 (2012) 956.
[9] R. Sànchez, J. M. Franco, M. A. Delgado, C. Valencia, and C. Gallegos, Carbohydr. Polym. 83 (2011) 151.
[10] C. Wang, Y. Dong, and H.Tan, J. Polym. Sci. A: Polym. Chem. 41 (2003) 273.
[11] D. Roy, J. T. Guthrie, and S. Perrier, Macromolecules 38 (2005) 10363.
[12] W. Yuan, J. Yuan, F. Zhang, and X. Xie, Biomacromolecules 8 (2007) 1101.
[13] K. R. Rao, P. Senapati, and M. K. Das, J. Microencapsul. 22 (2005) 863.
[14] J. Q. Gao, Q. Q. Zhao, T. F. Lv, W. P. Shuai, J. Zhou, G. P. Tang, W. Q. Liang, Y. Tabata, and Y. L. Hu, Int. J. Pharm. 387 (2010) 286.
[15] R. K. Malkani, K. S. Suresh, and G. V. Bakore, J. Inorg. Nucl. Chem. 39 (1977) 621.
[16] A. G. Fadnis, and S. K. Kulshrestha, React. Kinet. Catal. Lett. 19 (1982) 267.
[17] El-Mallah, A. Talaat, Abbas, M. Hassib, Shaffei, and M. Farid, Metal Finish. 86 (1988) 29.
[18] G. Y. Li, J. S. Lian, L. Y. Niu, and Z. H. Jiang, ISIJ Int. 45 (2005) 1326.
[19] F. B. Brahim, and H. Boughzala, J. Mol. Struct. 1034 (2013) 336.
[20] W. Ojczyk, J. Marzec, K. Swierczek, and J. Molenda, Defect Diffus Forum 237–240 (2005) 1299.
[21] V. Koleva, V. Stefov, A. Cahil, M. Najdoski, B. Šoptrajanov, B. Engelen, and H. D. Lutz, J. Mol. Struct. 917 (2009) 117.
[22] P. Kubáˇn, and P.C. Hauser, Anal. Chim. Acta 607 (2008) 15.
[23] M. Pumera, Talanta 74 (2007) 358.
[24] L. Coury, Curr. Sep. 18 (1999) 91.
[25] J. S. Daniels, and N. Pourmand, Electroanal.19 (2007) 1239.
[26] E. D. Trutman, and R. S. Newbower, IEEE Trans Biomed. Eng. 30 (1983) 141.
[27] P. Kubáˇn, and P. C. Hauser, Electrophoresis 30 (2009) 176.
[28] T. Arfin, F. Jabeen, and R. J. Kriek, Desalination 274 (2011) 206.
[29] T. Arfin, and Rafiuddin, Electrochim. Acta 54 (2009) 6928.
[30] T. Arfin, and Rafiuddin, Desalination 284 (2012) 100.
[31] T. Arfin, and Rafiuddin, Electrochim. Acta 55 (2010) 8628.

[32] T. Arfin, and Rafiuddin, Electrochim. Acta 56 (2011) 7476.
[33] T. Arfin, and N. Yadav, Anal. Bioanal. Electrochem. 4 (2012) 135.
[34] T. Arfin, R. Bushra, and R. J. Kriek, Anal. Bioanal. Electrochem. 5 (2013) 206.
[35] T. Arfin, and S. Fatima, Asian J. Adv. Basic Sci. 2 (2013) 1.
[36] R. Cruickshank, J.P. Duguid, B.P. Marmion, and R.H.A. Awain, 12th ed., Medicinal Microbiology, Vol. 11, Churchill Livingstone, London (1995).
[37] A. H. Collins, Microbiology Method, 2nd ed., Butterworth, London (1976).
[38] P. S. Kalsi, Spectroscopy of organic compounds, New Age International Publishers, 6th Edition, New Delhi (2009).
[39] G. G. Aloisi, and S. Pignataro, J. Chem. Soc. Faraday Trans. 69 (1973) 534.
[40] A. B. P. Lever, Inorganic Electronic Spectroscopy, 2nd ed., Elsevier, Amsterdam (1985).
[41] G. Briegelab, and J. Czekalla, Z. Phys. Chem. 24 (1960) 37.
[42] G. Briegleb, Angew. Chem. 76 (1964) 326.
[43] J. Desai, K. Alexander, and A. Riga, Int. J. Pharm. 308 (2006) 115.
[44] Y. Bai, C. Jiang, Q. Wang, and T. Wang, Carbohydr. Polym. 96 (2013) 522.
[45] C.N.R. Rao, Chemical Applications of Infrared Spectroscopy, Academic Press, New York (1963).
[46] S.A. Nabi, R. Bushra, M. Naushad, and A.M. Khan, Chem. Eng. J. 165 (2010) 529.
[47] N.M. Aghatabay, M. Tulu, Y. Mahmiani, M. Somer, and B. Dulger, Struct. Chem. 19 (2008) 71.
[48] M.N. Beg, K. Ahmad, I. Altaf, and M. Arshad, J. Membr. Sci. 9 (1981) 303.
[49] G. Eisenman, The glass electrode, Interscience, New York (1965).
[50] F. A. Siddiqi, N. Lakshminarayanaiah, and M. N. Beg, J. Polym. Sci. 9 (1971) 2853.
[51] T. Arfin, and F. Mohammad, J. Ind. Eng. Chem. 19 (2013) 2046.
[52] H. S. Nalwa, Handbook of advanced electronic and photonic materials and devices, Academic Press, New York (2001).
[53] C. A. Cumins, and T. K. Kwei, In: J. Crank, and G. S. Park (eds.), Diffusion in polymers, Academic Press, London (1968).
[54] U. Ishrat, and S. M. Rafiuddin, Eur. Chem. Bull. 3 (2014) 24.